

# Research Journal of Pharmaceutical, Biological and Chemical Sciences

## Thermodynamic And Kinetic Of Methylene Blue Adsorption On Synthesized and Modified Mesoporous Silica.

Noorah Abdul Kareem Khalaf, and Sameer H Kareem\*.

Department of Chemistry-College of Science-University of Baghdad, Iraq.

### ABSTRACT

Two samples of Mesoporous Silica (MPS) and modified Mesoporous silica (MPS-Cr) were prepared by the simultaneous hydrolysis and condensation of sodium silicate in the presence of HydroxycetylHydroxy ethyl Diamonium Chloride surfactant as template. The two adsorbents prepared were characterized by nitrogen adsorption-desorption, XRD and AFM techniques. The results show a high degree of ordering of the porous structure. The adsorption behavior of methylene blue (MB) from aqueous systems onto the two adsorbents has been studied using a batch experiments method to measure the adsorption as a function of contact time, adsorbent dose, and temperature (288, 298, 308 and 318 K). The equilibrium of the process was achieved within 120 min. The adsorption of methylene blue onto MPS and MPS-Cr was found to decrease with increasing temperature which indicates an exothermic process. Adsorption isotherms were fitted with the Langmuir, Freundlich, Temkin, and Dubinin –Radushkevich models. The kinetic data were analyzed and found to match well with pseudo-second order kinetic model. The thermodynamic of the process was also studied and the results indicate that the  $\Delta G^\circ$  and  $\Delta H^\circ$  were negative indicating the adsorption process was spontaneous and exothermic in nature.

**Keywords:** mesoporous silica, methylene blue, silica-Cr composite, adsorption isotherm

\*Corresponding author

## INTRODUCTION

Mesoporous silica (MPS) has attracted much interest in the recent years due to their potential in numerous fields including adsorption, sensing, catalysis and drug delivery applications. Such materials, characterized by a very high specific surface area and pore volumes, and ordered porous structure [1-4].

In 1992, researchers in Mobil Corporation laboratories published a series of ordered mesoporous silica with pore sizes ranging from 1.5-10 nm. The variant called MCM-41 with  $1000 \text{ m}^2\text{g}^{-1}$  surface area and pore volumes up to  $1 \text{ cm}^3\text{g}^{-1}$ , has been comprehensively studied and widely applied in many fields [5]. Templates with amphiphilic materials are usually used to synthesize MPS materials with ordered packed pore structures [6]. Also, block copolymers with much longer hydrophobic chain length than those used in the synthesis of MCM-41 have been used to template ordered pore materials with large pores [7].

In addition to preparation of various mesoporous silica structures, incorporation of heteroatoms such as Cu, Zn, Al, B, Ga, Fe, Cr, Ti, V, Sn etc. into MPS framework has been widely investigated. The template synthesis of MPS is extended to prepare various mesoporous metal oxides such as  $\text{TiO}_2$ ,  $\text{Ta}_2\text{O}_5$ ,  $\text{Nb}_2\text{O}_5$ ,  $\text{ZrO}_2$ ,  $\text{Al}_2\text{O}_3$ ,  $\text{V}_2\text{O}_5$  etc. [8-10].

In our laboratory, a various type of mesoporous silica as adsorbents was prepared and characterized using different techniques [11-13]. Adsorption from solution method was used to examine their adsorptive removal of some organic pollutants and study the kinetics and thermodynamic of the adsorption process.

The main objective of this work is to synthesize mesoporous silica, to modify it by addition of  $\text{Cr}_2\text{O}_3$ , and to evaluate the adsorption capacity of these mesoporous materials with respect to MB dye with a cationic character. A detailed study is presented defining the different methods of characterization. Thermodynamic and kinetic study and that of adsorption isotherms will also be discussed.

## EXPERIMENTAL

**Chemicals:** The materials used in the experiments were as follows: sodium silicate (14% NaOH, 27%  $\text{SiO}_2$ ) and HydroxyCetylHydroxy ethyl Diamonium Chloride (Dehyquart E-CA) were purchased from local market. Methylene blue and Hydrochloric acid was purchased from Fluka and BDH respectively.

**Characterization:** The resultant materials were characterized by XRD and  $\text{N}_2$  adsorption-desorption isotherms. The adsorption-desorption isotherms of  $\text{N}_2$  at 77 K were obtained using a Micromeritics ASAP 2020 Instrument. The X-ray diffraction (XRD) patterns were obtained with a Rigaku diffractometer using  $\text{Cu K}\alpha$  ( $\lambda = 0.154 \text{ nm}$ ) radiation.

### Preparation of Adsorbents

#### Preparation of MPS

An amount of HydroxyCetylHydroxy ethyl Diamonium Chloride (dehyquart) (3.7 g) was dissolved in 150 ml of distilled water, and put in a round bottom flask. 8.5 mL (1M)  $\text{H}_2\text{SO}_4$  was added and the mixture stirring for 1 hour. In 250 ml beaker, 7.5 g of sodium silicate was dissolved in 150 ml of distilled water and was added to the mixture drop by drop from burette for 3 hours. The white precipitation was formed and then it was recovered by filtration, washed with water, after aging for one day at  $80^\circ\text{C}$ . After drying at  $80^\circ\text{C}$  the surfactant was removed by calcinations at  $600^\circ\text{C}$  for 4 hours.

#### Preparation of MPS-Cr

MPS-Cr adsorbent is a composite of mesoporous silica ( $\text{SiO}_2$ ) and Chromium Oxide ( $\text{Cr}_2\text{O}_3$ ). The procedure is as follows and the optimum conditions used are as these used in preparation of (MPS) sample:

A mixture of sodium silicate solution (7.5g in 150ml distilled water), Dehyquart surfactant solution (3.7 g in 150 ml distilled water), and Chromium nitrate solution ( $\text{Cr}(\text{NO}_3)_3 \cdot 9\text{H}_2\text{O}$ ) (2.3g in 10 ml distilled water) were put in a round bottom flask. 35 ml of 5M nitric acid was added to the mixture drop by drop from burette for 3h.

**Adsorption procedure**

The adsorption isotherm was constructed using 100 ml of different MB concentration (10, 15, 20, 25, 30, 35, 40 mg/L) with 0.075g of adsorbent. These mixtures were shaken well for 120 minutes to reach equilibrium. A sample has been pipette and placed in the centrifuge for 10 minutes; the concentrations of the MB solution before and after the adsorption were determined by UV-Visible spectrophotometer at  $\lambda_{max}$  664nm. The amount of dye adsorbed was determined by the equation:

$$q_e = (C_0 - C_e)V / W \quad \text{----- (1)}$$

Where  $q_e$  is the equilibrium adsorption capacity of MB adsorbed on unit mass of the adsorbent (mg /g),  $C_0$  and  $C_e$  are the initial MB concentration ( $mg L^{-1}$ ) and at equilibrium respectively,  $V$  (L) is the volume of MB solution and  $W$  (g) is the weight of adsorbent.

The concentration of MB was measured and the percentage removal (R %) was determined according to the equation :

$$R\% = (C_0 - C_e) \times 100 / C_0 \quad \text{----- (2)}$$

The effect of temperatures on the removal of MB was studied using four temperatures in the range of (298-328) K using the thermostatic shaker bath.

**RESULTS AND DISCUSSION**

**Adsorbents characterization**

X-ray diffraction patterns in the  $2\theta$  range of 0-10 of synthesized samples MPS and its modification MPS-Cr are shown in Figure(1) respectively. The patterns show a single, well-resolved, strong diffraction peak at  $2\theta = 1.9323$  for MPS sample and  $2\theta = 1.2000$  for MPS-Cr sample which shows a high degree of ordering of the porous structure. This is attributed to the typical diffraction peak of mesoporous  $SiO_2$ [14]. Thus, it proved that deposition of  $Cr_2O_3$  species did not damaged the porous structure of the MPS support [15, 16]. Using the related data and Scherer equation ( $D = 0.9 \lambda / B \cos \theta$ ), where  $\lambda$  is wavelength of x-ray (Å),  $B$  is FWHM (radian) and  $\theta$  is position (radian), the diameter of the crystalline particles are 26.9 nm and 60.46 nm for MPS and MPS-Cr respectively.

The  $N_2$  adsorption - desorption isotherm for MPS sample(Fig. 2) shows that it can be considered type IV according to the common classification of adsorption isotherms. The hysteresis loop observed are typical for mesoporous materials and resemble the loops of type H1 according to the IUPAC classification which means that the adsorbent has a regular cylindrical pore without intersecting channels [17]. In addition, the pore size distribution result (Fig.2) confirms the presence of mesoporosity and have a narrow pore size distribution (from 2 to 50 nm).

Figure (3) shows the Histogram of Granularity Distribution for a) MPS and b) MPS-Cr using atomic force microscopy. We show that the diameter of the particles are in the range 65-145nm and average diameter of particles 87.64nm, for MPS sample while for MPS-Cr composite the figure shows that the particles in range 60-115 nm, and average diameter of particles 72.11nm. The results also show that about 83% and 97% of the particles were less than 100nm for the samples MPS and MPS-Cr respectively. Comparing the results, one can see that the granule size of MPS-Cr is smaller than the granule size of MPS.

**Adsorption behavior**

**Effect of adsorbent dose:** The experiments were conducted for 30 mg/L concentration of 100 mL MB dye solution with different amounts (0.010, 0.025, 0.050, 0.075, and 0.10 g) of adsorbents, the maximum dye removal was achieved within 120 minutes. Figure (4) shows the variation of percentage removal (R %) with the amount of adsorbent and the results show that the 0.075 g dose gives the best result with R% equal to 84.65% and 72.33 for MPS and MPA-Cr respectively. Therefore the adsorption experiments in this work were performed

with 0.075 g of the two adsorbent. Above this dose the percentage of removal was decreased which may be due to some factors such as: 1-the adsorption competition among the adsorbent, 2-splitting effect of concentration gradient between dye molecules and adsorbent concentration, 3-the adsorption site remains unsaturated during the adsorption process [18, 19].

**The effect of equilibrium time**

The effect of contact time on the adsorption of MB on MPS and MPS-Cr is illustrated in Figure (5) which shows the gradual increase in adsorption with increasing contact time up to 120 minutes in which a maximum value of adsorption is attained, so all the experiments of adsorption were done at this equilibrium time. In the initial stage, dye adsorbs quickly where the available active sites on the surface of MPS are large which cause a fast adsorption with increase in the contact time. The available active site was gradually decreased leading to the slow adsorption process and taking long time to reach adsorption equilibrium.

**Adsorption Isotherm**

The adsorption isotherm was constructed using 100 mL of MB solution at seven different concentrations (10, 15, 20, 25, 30, 35, 40 mg/L) with 0.07g of adsorbent at 298, 308, 318, and 328K. The amount of dye adsorbed was determined by the equation (1) while the R% calculated by equation (2), and the results obtained were listed in Table (1) and given in Figure (6).

The results of Figure (6) indicate that the adsorption capacity decrease with increasing temperature from 298-328 K showing that the adsorption of MB on MPS is exothermic. This can be explained that when the temperature increased; 1-the physical bonding between the dye molecules and the adsorbent weakened, 2-the solubility of MB dye increased which cause the interaction between adsorbate and adsorbent to decrease. So the Solute was more difficult to adsorb at higher temperature [20].

Three isotherms were analyzed to investigate the adsorption isotherm: Langmuir [21], Freundlich [22] and Temkin [23] as the following equations:

$$C_e/q_e = 1/(K_L q_m) + C_e/q_m \text{ ----- (3)}$$

$$\ln q_e = \ln K_F + 1/n \ln C_e \text{ ----- (4)}$$

$$q_e = B \ln K_T + B \ln C_e \text{ ----- (5)}$$

Where,  $K_L$ ,  $K_F$ , and  $K_T$  are Langmuir isotherm constant (L/mg), Freundlich isotherm constant (mg/g), and the Temkin isotherm constant respectively.  $q_m$  is maximum monolayer coverage capacity (mg/g).  $n$  is dimensionless constant related to the intensity of adsorption, or the heterogeneity factor and is not restricted to the formation of the monolayer.  $B$  is a constant equal to  $RT/b_T$ ;  $b_T$  is corresponding to heat of adsorption,  $R$  is the universal gas constant and  $T$  is Temperature.  $q_m$  and  $K_L$  are determined from the intercept and slope of plots of  $C_e/q_e$  versus  $C_e$ ,  $n$  and  $K_F$  are determined from the intercept and slope of plots of  $\ln q_e$  versus  $\ln C_e$ , and  $B$  and  $K_T$  are determined from the intercept and slope of plots of  $q_e$  versus  $\ln C_e$ . The best fit model was selected based on the linear regression correlation coefficient values ( $R^2$ ). The results of such plots are tabulated in Table (2).

From Table (2), the values of  $K_F$  show that the uptake of MB decreases with increase in temperature indicating the exothermic nature of the adsorption process studied. The values of  $n$  are more than 1 suggesting favorable adsorption of MB on MPS and MPS-Cr. When the value of  $n$  in the range ( $1 < n < 10$ ) as well as  $0 < 1/n < 1$  indicating it is satisfying the condition of heterogeneity and positive cooperatively [24].

The results of Table ( 2 ) also show that the experimental data fitted well to the three adsorption models Langmuir, Freundlich and Temkin, but the Freundlich and Temkin models are slightly better fit to the data than Langmuir models because the correlation coefficient [ $R^2$ ] values of Langmuir model are lower than those for Freundlich and Temkin models.

Dubinin-Radushkevich isotherm is another isotherm equation that applied in this study to predict the type of adsorption. For solid-liquid interaction the linear form of Dubinin–Radushkevich (D–R) isotherm (equation 4) can be written as follows [25]:

$$\ln q_e = \ln q_m - \beta \varepsilon^2 \dots \dots (6)$$

Where  $\varepsilon$  is the Polanyi potential which equal:

$$\varepsilon = (1 + 1/C_e) \dots \dots \dots (7)$$

$\beta$  is a constant related to the adsorption energy ( $\text{mol}^2 \text{kJ}^{-2}$ ). The D-R model is important for predicting the nature of adsorption process through the determination of the mean adsorption energy (E) using equation [26]:

$$E = 1 / \sqrt{2\beta} \dots \dots \dots (8)$$

The mean adsorption energy E calculated from D-R model for the two adsorbents are in the range 1.00 - 2.272 kJ/mol which reveals that the adsorption of MB onto MPS and MPS-Cr was dominated physical adsorption since all values of E are less than  $8 \text{kJmol}^{-1}$  [27].

**Kinetics Study:** Three kinetic models are used; Lagergren-first-order [28], pseudo-second order [29], and Intra-particle diffusion model of Weber and Morris [30] equations which can be expressed as:

$$\ln q_e - q_t = \ln q_e - k_1 t \dots \dots \dots (9)$$

$$t / q_t = 1 / (k_2 q_e^2) + (1 / q_e) t \dots \dots \dots (10)$$

$$q_e = k_d t^{1/2} + C \dots \dots \dots (11)$$

Where  $k_1 (\text{min}^{-1})$ ,  $k_2 (\text{g mg}^{-1} \text{min}^{-1})$ , and  $k_d (\text{mg g}^{-1} \text{min}^{-1/2})$  are the rate constants of the pseudo-first order, pseudo-second order, and intra-particle diffusion kinetics respectively.  $q_e$  and  $q_t$  are the amounts of MB adsorbed on the surface of the adsorbent at equilibrium and at any time ( $\text{mg g}^{-1}$ ) respectively, C is constant.  $q_e$  and  $k_1$  are calculated from the intercept and the slope of plots of  $\log (q_e - q_t)$  vs  $t$  (Fig. 7),  $k_2$  and  $q_e$  are calculated from the intercept and the slope of plots of  $t/q_t$  against  $t$  (Fig. 8), ( $k_d$ ) can be estimated from the slope of the linear plot of the amount of solute adsorbed ( $q_e$ ) against square root of time ( $t^{1/2}$ ) (Fig. 9).

These models have been used to research the adsorption kinetic behavior of MB (30 mg/L) onto MPS and MPS-Cr. The best fit model was selected based on the linear regression correlation coefficient values ( $R^2$ ). The results of such plots are tabulated in Table (3).

From results in Table (3) the correlation coefficient ( $R^2$ ) values obtained from pseudo-second order kinetic model was higher than that of pseudo first-order which indicate that the adsorption perfectly complies with pseudo-second order model. Also, it can be seen from the plot of intra-particle diffusion model, the adsorption was controlled by two stages. The first linear portion was a gradual adsorption where intraparticle diffusion was the rate determining factor. The second linear portion was the equilibrium stage due to low concentration of surfactant in the solution phase. As can be seen in the plot, the intraparticle diffusion was not the rate determining factor as the first linear portion of the plot did not pass through the origin [31,32].

**Thermodynamics Analysis**

The standard free energy change ( $\Delta G^\circ$ ), enthalpy change ( $\Delta H^\circ$ ) and entropy change ( $\Delta S^\circ$ ) were determined using the following equations [33]:

$$\Delta G^\circ = -RT \ln K_{eq} \dots \dots \dots (12)$$

$$\ln K_{eq} = \Delta S^\circ / R - \Delta H^\circ / RT \dots \dots \dots (13)$$

where  $K_{eq}$  is the equilibrium constant which is calculated from the following equation:

$$K_{eq} = q_e(\text{mg/kg}) / C_e(\text{mg/L}) \quad \text{----- (14)}$$

The slope and intercept of the van't Hoff plot is equal to  $-\Delta H/R$  and  $\Delta S^{\circ}/R$  in which the thermodynamic parameters obtained are summarized in Table (4).

The negative values of  $\Delta G^{\circ}$  obtained on the adsorption of MB on the two adsorbents indicate the spontaneous nature of sorption. This suggests high preference of methylene blue for MPS and MPS-Cr. The negative values of adsorption enthalpy in the case of the two adsorbents show that the adsorption process is exothermic. The positive values of  $\Delta S^{\circ}$  indicate the decrease in the order of the system.

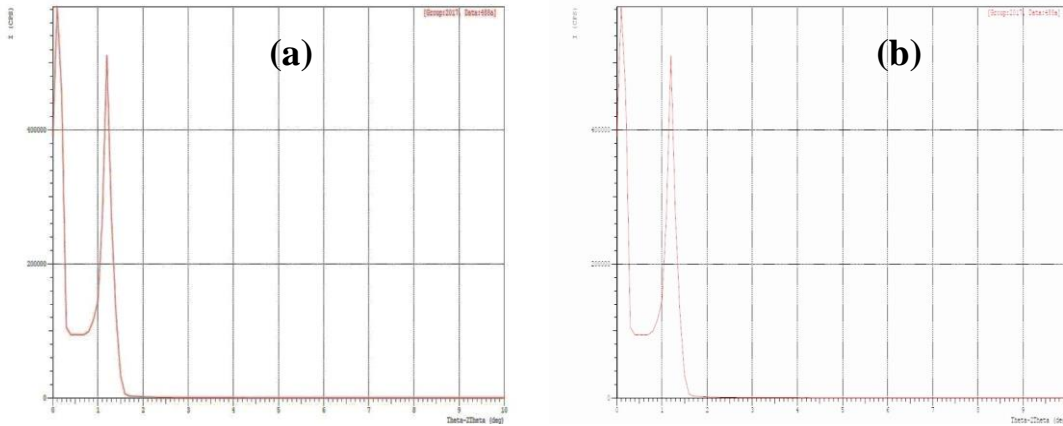


Figure 1. XRD Patterns of (a) MPS, (b) MPS-Cr after calcinations in 2θ range (0-10).

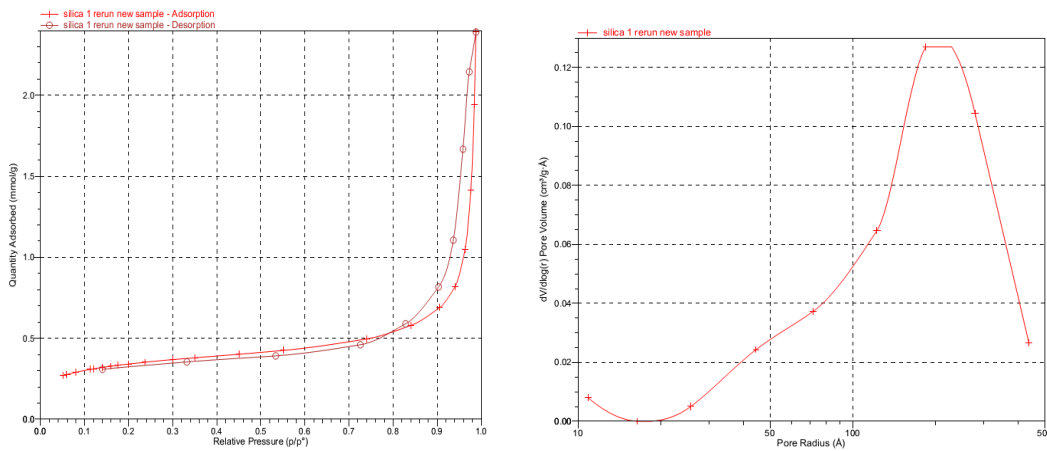


Figure (2) a) N<sub>2</sub> adsorption-desorption isotherm b) PZD for MPS sample.

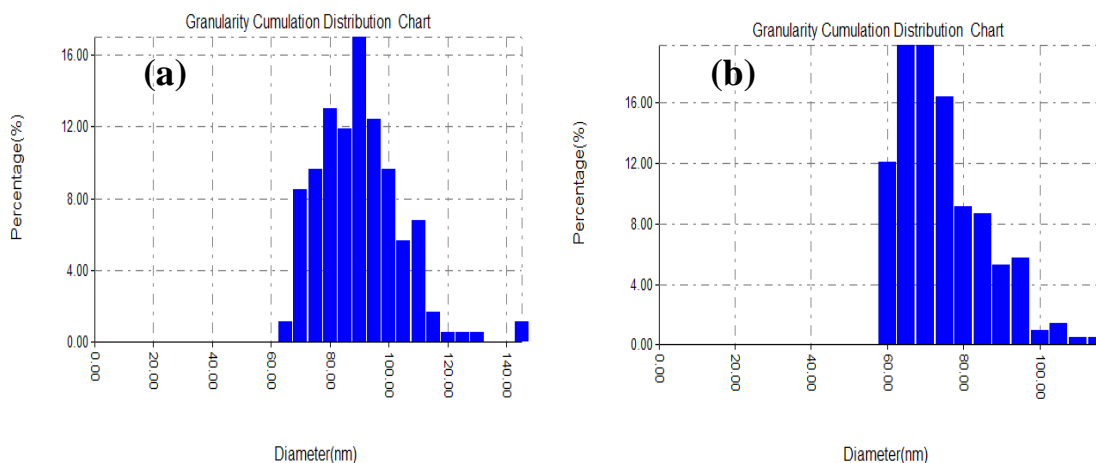


Figure (3): Histogram of Granularity Distribution for (a) MPS and (b) MPS-Cr.

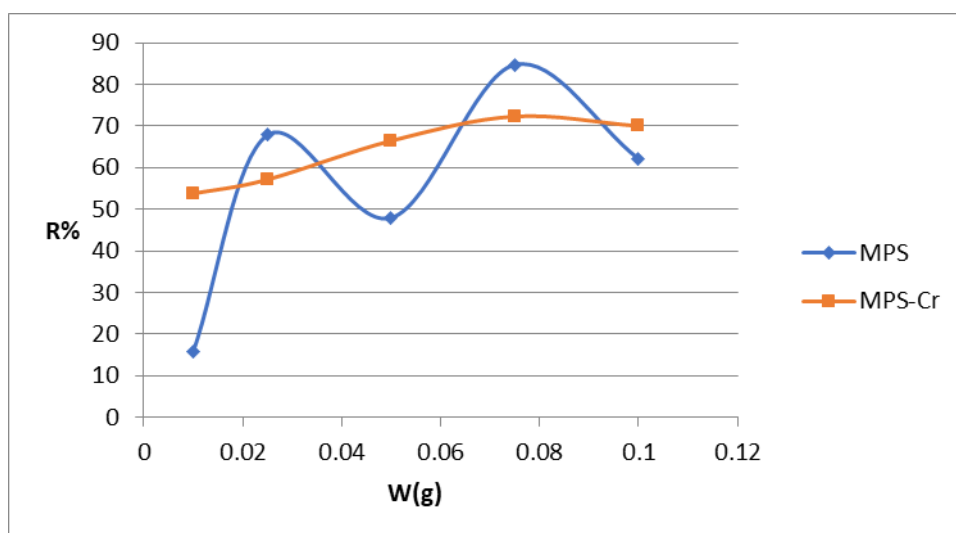


Figure 4. The value of R% and quantity of MPS and MPS-Cr adsorbents for adsorption of MB ( $C_0=30\text{mg/L}$ ,  $T=298\text{ K}$ ).

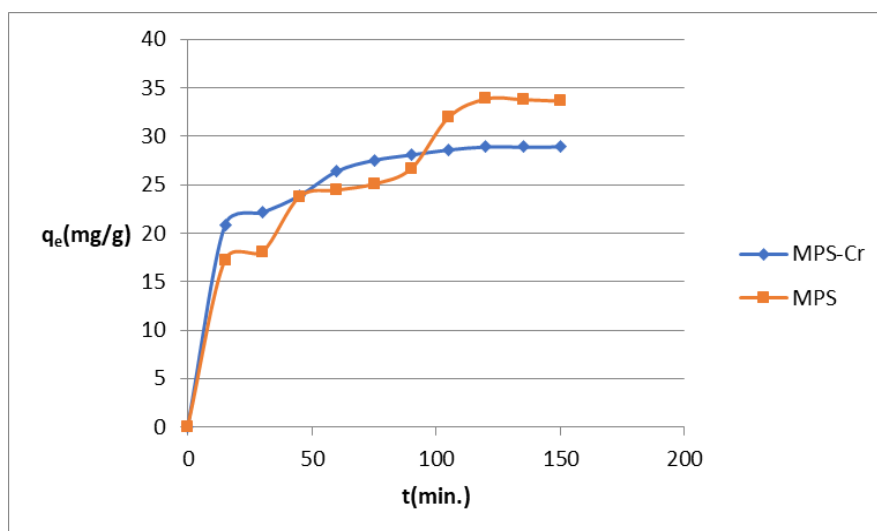


Figure 5. The effect of contact time on  $q_e$  and  $C_e$  for MB adsorption for MPS and MPS-Cr ( $C_0 = 30\text{mg/L}$ ,  $T=298\text{ K}$ ).

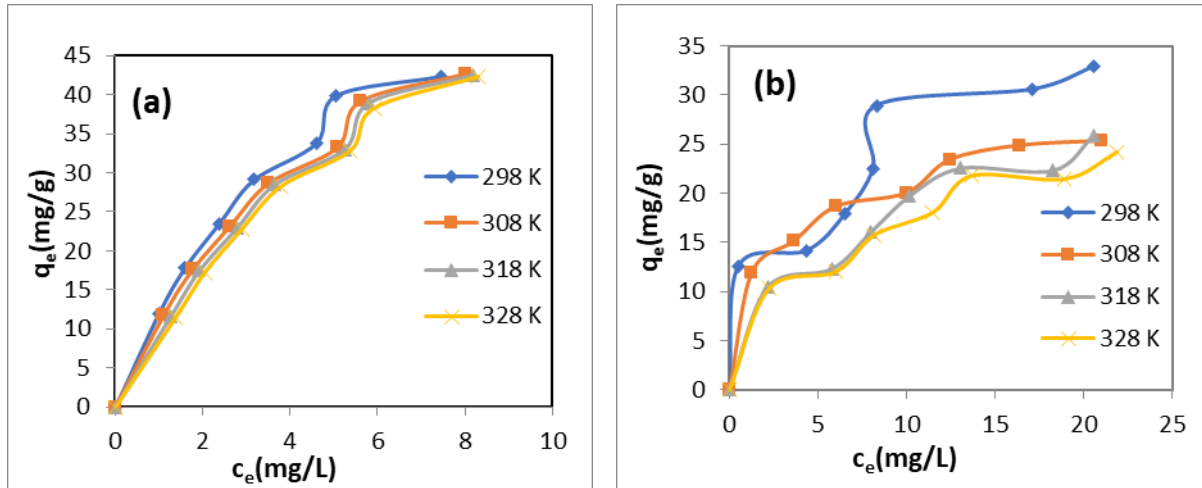


Figure 6. Adsorption isotherms for the adsorption of MB on (a) MPS and (b) MPS-Cr at different temperatures.

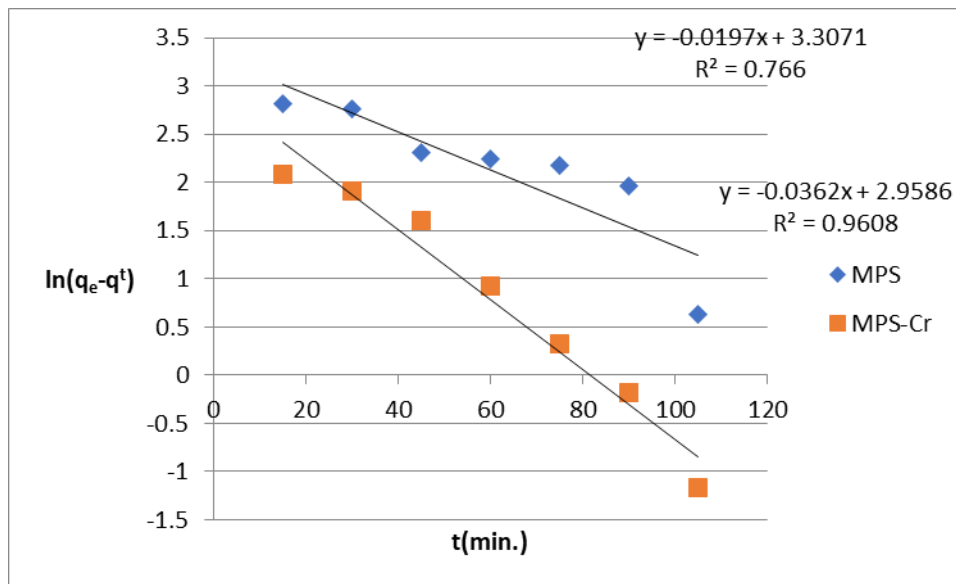


Figure (7): The pseudo-first order kinetic plot for adsorption of MB on MPS and MPS-Cr at 298 K.

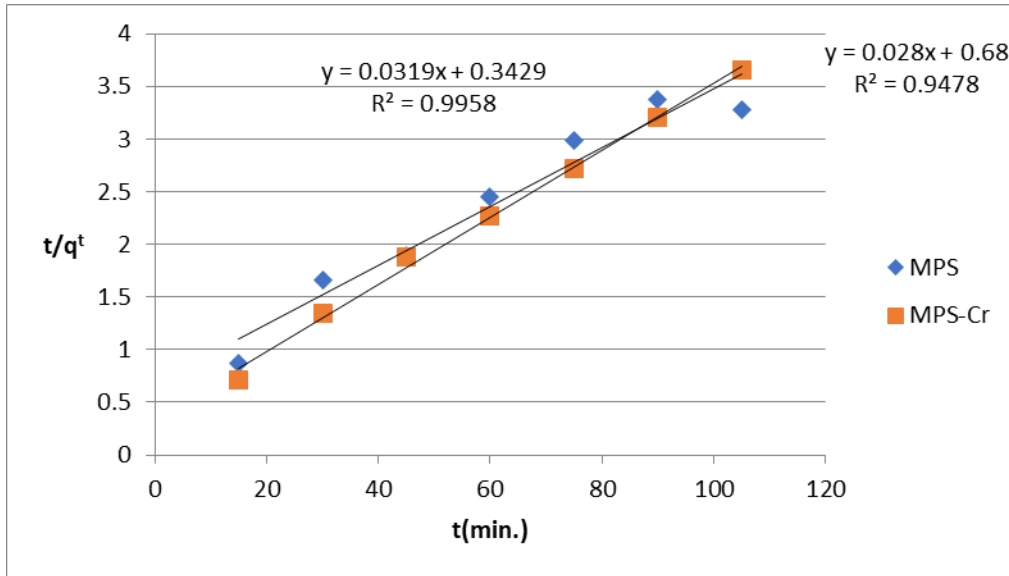


Figure 8. The pseudo-second order kinetic plot for adsorption of MB on MPS and MPS-Cr at 298 K.

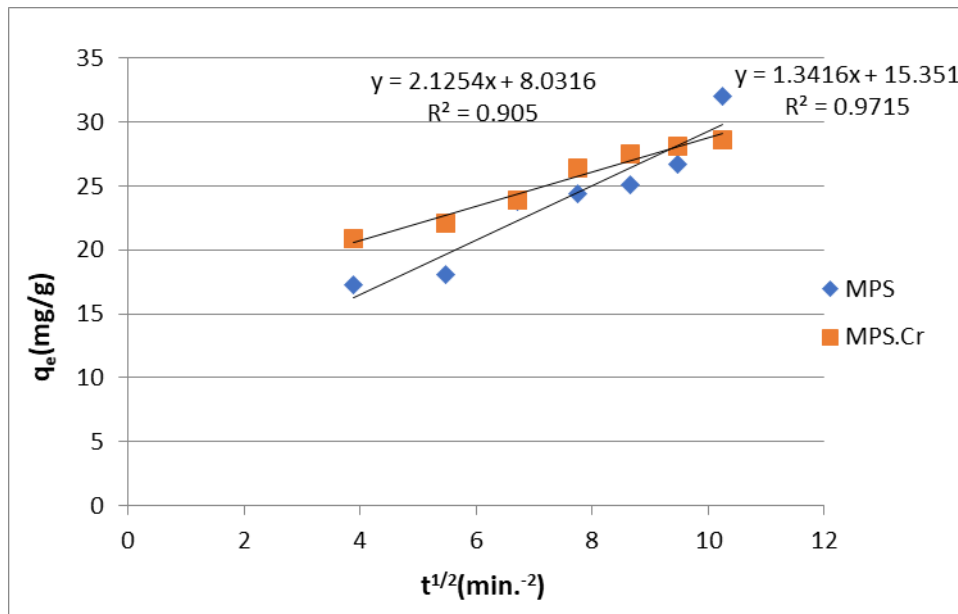


Figure 9. The intra-particle diffusion model for the adsorption of MB on MPS and MPS-Cr at 298 K.

Table 1. The values of C<sub>e</sub> and q<sub>e</sub> for the adsorption of MB on MPS and MPS-Cr at different temperatures.

sample	C <sub>0</sub> mg/L	298 K		308 K		318 K		328 K	
		C <sub>e</sub>	q <sub>e</sub>						
		mg/L	mg/g	mg/L	mg/g	mg/L	mg/L	mg/L	mg/L
	10	1.00	12.0	1.11	11.85	1.27	11.64	1.38	11.49
	15	1.60	17.87	1.77	17.64	1.93	17.44	2.05	17.26

MPS	20	2.38	23.50	2.62	23.17	2.79	22.94	2.90	22.80
	25	3.17	29.11	3.50	28.66	3.65	28.46	3.80	28.26
	30	4.61	33.86	5.07	33.24	5.25	33.00	5.38	32.82
	35	5.06	39.92	5.61	39.18	5.81	38.92	5.93	38.76
	40	7.46	42.39	8.00	42.66	8.18	42.42	8.31	42.25
MPS-Cr	10	0.53	12.62	1.26	11.92	2.15	10.46	2.25	10.33
	15	4.38	14.16	3.65	15.13	5.77	12.30	6.00	12.00
	20	6.54	17.94	6.01	18.65	7.97	16.04	8.18	15.76
	25	8.09	22.54	9.98	20.02	10.17	19.77	11.47	18.04
	30	8.30	28.93	12.44	23.41	13.06	22.58	13.66	21.78
	35	17.08	30.56	16.35	24.86	18.24	22.34	18.91	21.45
	40	20.53	32.86	21.01	25.32	20.55	25.93	21.86	24.18

Table 2. The parameters of Langmuir, Freundlich and Temkin models for adsorption of MB on MPS at different temperatures.

Adsorbent	T/ K	Langmuir model				Freundlich model			Temkin model		
		$q_m$	$K_L$	$R_L$	$R^2$	$n$	$K_F$	$R^2$	$B$	$K_T$	$R^2$
MPS	298	77.01	5.50	0.0052	0.969	1.54	12.88	0.975	15.99	1.97	0.980
	308	76.92	5.84	0.005	0.977	1.52	11.84	0.982	16.09	1.73	0.982
	318	83.33	7.33	0.004	0.960	1.42	10.68	0.975	16.85	1.43	0.948
	328	90.90	8.72	0.003	0.938	1.37	9.93	0.976	17.64	1.32	0.985
MPS-Cr	298	40.00	0.192	0.672	0.907	3.62	12.69	0.975	5.67	1.58	0.737
	308	29.41	0.311	0.718	0.993	3.24	10.26	0.989	5.51	1.88	0.974
	318	33.33	0.144	0.406	0.934	2.36	6.97	0.925	7.00	9.58	0.974
	328	31.25	0.140	0.877	0.941	2.50	6.88	0.935	6.33	6.35	0.902

Table (3): Kinetic parameters for adsorption of MB on MPS and MPS-Cr at 298 K.

MPS			MPS-Cr		
model	parameters	The value	model	parameters	The value
Pseudo first order	$q_e / \text{mg g}^{-1}$	2.72	Pseudo first order	$q_e / \text{mg g}^{-1}$	2.71
	$k_1 / \text{min}^{-1}$	0.019		$K_1 / \text{min}^{-1}$	0.036
	$R^2$	0.766		$R^2$	0.960
Pseudo second order	$q_e / \text{mg g}^{-1}$	35.71	Pseudo second order	$q_e / \text{mg g}^{-1}$	32.25
	$k_2 / \text{mg g}^{-1} \text{min}^{-1}$	0.0005		$K_2 / \text{mg g}^{-1} \text{min}^{-1}$	0.0003
	$R^2$	0.947		$R^2$	0.995
Diffusion	$K_d /$	2.125	Diffusion	$K_d$	1.341

model	$\text{mg g}^{-1}\text{min}^{-1/2}$		model	$\text{mg g}^{-1}\text{min}^{-1/2}$	
	$R^2$	0.905		$R^2$	0.971

Table 4. Thermodynamic parameters of MB adsorption on MPS and MPS-Cr.

MPS							MPS-Cr						
C <sub>0</sub>	$-\Delta H^\circ$ kJmol <sup>-1</sup>	$\Delta S^\circ$ Jmol <sup>-1</sup> K <sup>-1</sup>	$-\Delta G^\circ$ kJ.mol <sup>-1</sup>				C <sub>0</sub>	$-\Delta H^\circ$ kJmol <sup>-1</sup>	$\Delta S^\circ$ Jmole <sup>-1</sup> K <sup>-1</sup>	$-\Delta G^\circ$ kJ mole <sup>-1</sup>			
			298 K	308 K	318 K	328 K				298 K	308 K	318 K	328 K
10	10.14	44.03	23.2	23.7	24.1	24.5	10	43.56	64.66	24.9	22.8	22.4	22.9
15	7.73	51.41	23.1	23.5	24.1	24.6	15	17.20	10.95	20.0	21.4	20.2	20.7
20	6.15	55.67	22.7	23.2	23.8	24.4	20	11.72	27.17	19.6	20.5	20.0	20.6
25	5.48	57.21	22.5	23.1	23.6	24.2	25	14.02	18.22	19.6	19.4	20.0	20.1
30	4.90	57.17	22.1	22.4	23.1	23.7	30	8.81	34.21	19.1	19.2	19.7	20.1
35	4.99	57.47	22.2	22.6	23.2	23.9	35	12.88	18.86	18.5	18.7	18.7	19.1
40	2.90	61.96	21.4	21.9	22.6	23.2	40	8.48	32.25	18.2	18.1	18.8	19.1

### CONCLUSIONS

the foregoing results of XRD and PZD indicate the presence of mesoporosity in the two samples prepared and have a narrow pore size distribution (from 2 to 50 nm). The results of AFM show the diameter of the particles are in the range 65-145 nm and average diameter of particles 87.64 nm, for MPS sample while for MPS-Cr composite the figure shows that the particles are in the range 60-115 nm, and average diameter of particles 72.11 nm. The results also show that about 83% and 97% of the particles were less than 100 nm for the samples MPS and MPS-Cr respectively. The study of MB adsorption on the two adsorbents shows the adsorption is physisorption which is reflected by the values of  $\Delta H^\circ$  obtained and D-R equation. Kinetics investigation has reflected that pseudo-second order kinetics equation is found as the best model for fitting kinetics data and intraparticle diffusion model is necessary through rate determining step reaction. Thermodynamic data results obtained has indicated that the adsorption processes are spontaneous and exothermic in nature.

### REFERENCES

- [1] Karakassides, M. A., Bourlinos, A., Petridis, D., Coche-Guerente, L., and Labbe, P., *J. Mater. Chem.*, 2000; 10(2): 403-408.
- [2] Kresge, C. T., Leonowicz, M. E., Roth, W. J., Vartuli, J. C., and Beck, J. S., *Nature*, 1992; 359: 710-712.
- [3] Das, P., Silva, A., Carvalho, A., Pires, J., and Freire, C., *J. Mater. Sci.*, 2009; 44 (11): 2865-2875.
- [4] Daniel, M., Zofia, P., Karolina, T., Kinga Góra-M., Janusz, R., Lucjan, C., *Materials Research Bulletin*, 2016; 74: 425-435.
- [5] Beck, J.S., Vartuli, J.C., Roth, W.J., Leonowicz, M. E., Kresge, C. T., Schmitt, K. D., Chu, C. T. W., Olson, D. H., Sheppard, E. W., McCullen, S. B., Higgins, J. B., and Schlenker, J. L., *J. Am. Chem. Soc.*, 1992; 114(27): 10834-43.
- [6] Lin, H.P., and Mou, C.Y., *Acc. Chem. Res.*, 2002; 35: 927-935.
- [7] Ryoo, R., Ko, C.H., Kruk, M., Antochshuk, V., and Jaroniec, M., *J. Phys. Chem. B*, 2000; 104 (48): 11465-11471.
- [8] Nasir, V. D. and Sadhana, R., *Asian Journal of Pharmaceutical and Clinical Research*, 2011, 4(2).

- [9] Vinu A, and Hartmann M., ChemLett, 2004; 33: 588- 589.
- [10] Subramanian V, Jiang JC, Smith PH, Rambabu B., J NanosciNanotechnol, 2004; 4: 125- 131.
- [11] Sameer H. Kareem, Inaam H. Ali and M.G. Jalhoom, American Journal of Environmental Science, 2014; 10 (1): 48-60.
- [12] Sameer H. Kareem and Qutban Ibrahim, International Journal of Science and Research, 2016; 5 (1): 480.
- [13] Qutban Ibrahim, Inaam H. Ali, Sameer H. Kareem, International Journal of Science and Research, 2016; 5 (12): 1536.
- [14] Xiang Wei-Dong, Yang Yu-Xiang ,Chen Jing ,Wang Zhaolun, and Liu Xiang-Nong, J. Am. Ceram. Soc., 2008; 91(5): 1517–1521.
- [15] Y. Su, Y.-M.Liu, L.-C.Wang, M. Chen, Y. Cao, W.-L. Dai, H.-Y. He, K.-N.Fan, App. Catal. A: Gen., 2006;315 :91–100.
- [16] O. Aktas, S. Yasyerlia, G. Dogua, T. Dogu, Mater. Chem. Phys., 2011;31 :151–159.
- [17] Rouquerol J. D. Avnir C.W.,Fairbridge D.H., Everett and J.H. Haynes, Pure Appl. Chem.,1994; 66: 1739-1758.
- [18] Arani M., N.Yousef,Limaee, N.M.Mahmoodi ,andN.SalamanTabrizi, J.Colloid. Inter.Sci., 2005; 288: 371.
- [19] Namasivayam C. and Yamuna RT, E.nviron.Pollut., 1995; 89: 1.
- [20] Bilal A., Murat E. M., and Mustafa U, Turkish Journal of Chemistry ,2014; 1-16.
- [21] Langmuir, J. Amer. Chem. Soc., 1918; 40(9): 1316-1403.
- [22] FreundlichH.M.F., J. Phys. Chem., 1906; 57: 385-470.
- [23] Temkin M. I.; V. Pyzhev, Acta Phys. Chim. USSR, 1940; 12: 327–356.
- [24] Leila T., Behdad G., Ashtianib E. A., Nourali M., Desalination and Water Treatment, 2012; 44 : 118–127.
- [25] M.M Dubinin., Chem. Rev., 1960; 60:235-266.
- [26] CleitonA., E. Nunes, C. Mário, and Guerreiro., Quim. Nova, 2011; 34(3): 472-476.
- [27] ShireenI. H., National Journal of Chemistry, 2009; 35:415-426.
- [28] LagergrenS., Handlingar, 1898; 24(4):1-39.
- [29] McKayG., and Y.S. Ho. Biochem., 1999; 34: 451-465.
- [30] WeberW.L., and J.C. Morris, J. San. Eng. Div. ASCE, 1963; 89:31-39.
- [31] NiharR. B., and P. Santanu, Ind. Eng. Chem. Res., 2010; 49:7060–7067.
- [32] Abdul SalamJ., and N.Das, International Journal of Pharmacy and Pharmaceutical Sciences, 2013; 5(3): 987-993.
- [33] C. Pinghuo, Z. Xuezhen,; L. Yongxiu,; and L. Dongping, Applied Mechanics and Materials, 2014; 5:1311-1319.